Physicochem. Probl. Miner. Process., 54(2), 2018, 321-333

http://www.journalssystem.com/ppmp

Physicochemical Problems of Mineral Processing

ISSN 1643-1049

Received October 16, 2016; reviewed; accepted May 7, 2017

Physicochemical study of dye removal using electro-coagulation-flotation process

Fouad I. El-Hosiny [1], Mohamed A. Abdel-Khalek [2], Khaled A. Selim [2], Inge Osama [2]

[1] Ain Shams University, Faculty of Science, Cairo, Egypt

[2] Central Metallurgical Research & Development Institute (CMRDI), Cairo, Egypt

Corresponding author: kalekma@yahoo.com (M.A. Abdel Khalek)

Abstract: The performance of electro-flotation with aluminum electrodes for the removal of different dyes from synthetic aqueous solutions and real wastewater was studied. Parameters affecting the electro-coagulation-flotation process, such as pH, initial dye concentration, treatment time and temperature were investigated. The maximum dye removal from synthetic solutions was achieved at pH 7. The order of the dye removals is nonionic>cationic>anionic. The removal process follows pseudo first-order kinetics and the adsorption follows both physical and chemical adsorptions which is exothermic. Negative values of entropy change, $\Delta S°$, and Gibbs free energy change, $\Delta G°$, indicate that this adsorption process is spontaneous and less favorable at high temperatures. Treatment of a real wastewater from textile dyeing factory showed that the removal efficiency was ranging between 92-99% for all constituents. The energy consumption is 0.0167 kWh/dm^3.

Keywords: *electro-flotation, electrocoagulation, dyes, wastewater, kinetics, thermodynamics*

1. Introduction

Many industries, such as textile, paper, printing, leather, food, cosmetics, etc., use dyes to color their products, which generate a considerable amount of colored wastewater. The dyeing material poses a major problem to wastewater sources (Sleiman et al., 2007; Shah et al., 2013). Textile industry produces 5000 tons of dyeing materials and they are discharged into the environment every year. These poisonous materials absorb the oxygen from water (Mahmoodi et al., 2009; Pirkaramia et al., 2013). Nowadays, treatment of colored wastewater is of a great concern, because many dyes and their degradation products are toxic and carcinogenic, posing a serious hazard to aquatic living organisms (Garg et al., 2004; Crini et al., 2006). Generally, treatment of dye effluents can be classified into biological, chemical and physical treatment. Among all these processes, electrocoagulation or electro-flotation is a very well-known electrochemical technique, and has been found to be an attractive alternative for the treatment of textile dyes (Muthukumar et al., 2010; Morsi et al., 2011; Al-Shannag et al., 2012; Lemlikchi et al., 2012).

Electro-flotation is an emerging technology that combines the functions and advantages of conventional coagulation, flotation, and electrochemistry in wastewater treatment. Electro-flotation was studied extensively in the latter half of the 20th century, but at that time, it was not found to be widely feasible for water treatment. This was mainly due to the high electricity and investment costs (Chen, 2004). Meanwhile, the demand for high quality drinking water is increasing globally. Therefore, it has become necessary to develop more effective treatment methods for water purification and enhance the operation of current methods (Ville et al., 2013). Electro-flotation has many benefits as, compatibility, amenability to automation, cost effectiveness, energy efficiency, safety, and versatility (Abdel Khalek et al., 2003; Nandi et al., 2017).

The electro-flotation process operates on the basis of the principle that the cations produced electrically from iron or aluminum anodes which is responsible for the coagulation of contaminants

http://dx.doi.org/10.5277/ppmp1825

from an aqueous medium (Chaturvedi, 2013). The consumable metal anodes are used to continuously produce polyvalent metal cations in the region of the anode. These cations neutralize the negative charge of the particles moved towards the anodes by polyvalent cations from the anodes (iron or aluminum) (Ahmed et al., 2015). The process involves formation of coagulants by destabilization of the contaminants and aggregation of the destabilized phase to form flocks. Destabilization of contaminants would take place through compression of the diffuse double layer around the charged ions by anodic counter ions. These counter ions neutralize ionic species in the wastewater and reduce the electrostatic repulsion so that Van der Walls attraction predominates hence coagulation occurs which approach to the zero net charge (Elksibi et al., 2014). The flocculated particles are attracted by small bubbles of oxygen and hydrogen generated from electrolysis of water. Thus the flocculated particles float towards the surface (Sahu et al., 2014). Other physiochemical and electrochemical processes were also reported (Thirugnanasambandham et al., 2013 and 2014; Vasudevan et al., 2014).

This paper investigated the kinetics and thermodynamics of electro-coagulation-flotation of different dyes, such as anionic, cationic and nonionic from synthetic aqueous solutions and a real wastewater from textile dyeing factory.

2. Materials and Methods

2.1. Chemicals

Acid Red 1 (anionic), Basic Violet 3 (cationic) and Disperse Blue 14 (nonionic) dyes were of an analytical grade; 99.9% purity (Sigma-Aldrich and Merck). Their chemical structures are presented in Fig.1. The pH was adjusted by 0.01 M solutions of HCl and NaOH when required. The real wastewater was obtained from a textile factory.

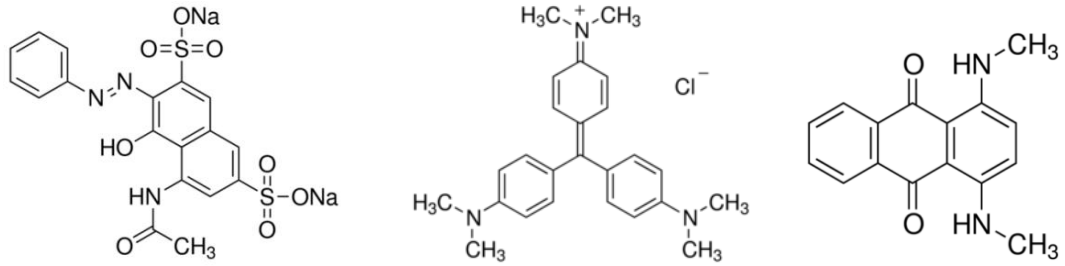

Acid Red 1 *Crystal Violet (Basic Violet 3)* *Disperse Blue 14*

Fig. 1. Chemical structures of different dyes used in this study

2.2. Procedure

A laboratory model DC power supply apparatus (Farnell Instruments LTD) was used to maintain a constant DC current. Voltage and current were measured by a multimeter (PHYWE). The pH and the temperature were measured using a Hanna (HI8314) pH meter.

Table 1. Chemical composition of 5052 aluminum alloy

Element	%
Magnesium	2.47
Chromium	0.23
Copper	0.06
Iron	0.34
Manganese	0.07
Silicon	0.19
Zinc	0.04
Aluminum	96.6

Electro-coagulation-flotation was conducted in a cylindrical glass cell of 400 cm^3 in which aliquot solutions of 300 cm^3 were placed and slowly stirred with a magnetic bar at 120 rpm. Schematic

diagram of electro-coagulation-flotation cell is provided in Fig. 2. In the experiments, a pair of commercially obtained aluminum plates (alloy 5052) of size 6 cm × 5 cm × 0.5 cm are used, immersed to 6 cm depth with an effective area of 30 cm^2. Chemical composition of the used alloy can be seen in Table 1. The inter-electrode distance was 4 cm. A 0.2% KCl was added for preventing passivation on the aluminum electrode surface and decreasing excessive ohmic drop in the solution. The residual dye concentrations were determined by UV/Vis spectrophotometer (LLG-UniSPEC 2).

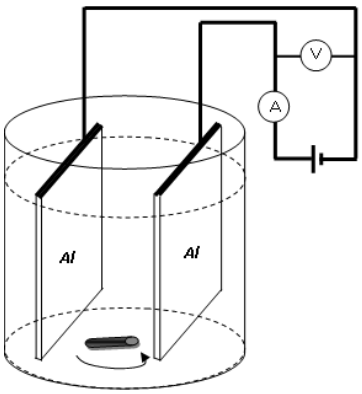

Fig. 2. Schematic diagram of electro-coagulation-flotation cell

The removal percent and the dye amount adsorbed on $Al(OH)_3$ (q_e) were calculated by Equations 1 and 2, respectively (Hunsom et al., 2005; Mohora et al., 2012):

$$Removal\ (\%) = \frac{C_0 - C_t}{C_0} \times 100, \tag{1}$$

where C_0 and C_t are the concentrations of dye solution (mg/dm^3) at time zero and t, respectively and:

$$q_e = \frac{(C_0 - C_t)\,V}{M}, \tag{2}$$

where q_e is the sorption capacity of $Al(OH)_3$ in g/g, V is the volume of the dye solution in L and M is the mass of $Al(OH)_3$ in g which calculated by (Konstantinos et al., 2011):

$$m\ Al(OH)_3 = \frac{I.t.M}{z\ .F}, \tag{3}$$

where I is current intensity (A), t is time (s), M is molecular weight of aluminum hydroxide (g/mol), z is the number of electrons transferred in the reaction $Al \rightarrow Al^{3+} + 3e$, and F is the Faraday's constant (96500 Cb/mol).

Chemical Oxygen Demand (COD) and Biochemical Oxygen Demand (BOD) is an empirical test that determines the relative oxygen requirements of wastewater, effluent and polluted waters using the respirometric method. The sample bottle is connected to a pressure sensor in a closed system. As bacteria consume oxygen in the sample the pressure in the bottle drops. This pressure change correlates directly to BOD. The most common BOD test consists of a 5-day period in which a sample is placed in an airtight bottle under controlled conditions temperature (20°C ± 1°C), keeping any light from penetrating the sample to prevent photosynthesis. TS (Total solid), TSS (Total suspended solid) and heavy metals were measured according to Standard Methods (Cleceri et al., 1998). Total solids are measured by evaporating all of the water out of a sample and weighing the remaining solids. Suspended solids are measured by passing sample water through a filter. The solids caught by the filter, once dried, are the suspended solids. Heavy metals were measured by Perkin Elmer, AAanalyst atomic absorption. Turbidity was recorded on a 2100N IS Turbidimeter (Hach). Color was determined by absorption scan (190–350 nm) using UV/Vis-Spectrophotometer (LLG-UniSPEC 2) (APHA, 1992).

3. Results and discussion

3.1. Effect of pH

The pH is an important factor for removal efficiency of dyes, so the initial pH was investigated for its effect on the removal percentage. The removal mechanism of pollutants is based on their adsorption

on the $Al(OH)_3$ flocs. Fig. 3 shows that the pH affects $Al(OH)_3$ stability in the solution (Basiri Parsa et al., 2011). It demonstrates different forms of $Al(OH)_3$ relative to the pH and concentration of Al^{3+} ions in the media (Jiang et al., 2002). In the high and low pH, $Al(OH)_3$ is in its charged form and is soluble in water, hence, cannot be used for electro-coagulation-flotation. But in neutral pH, $Al(OH)_3$ is stable and insoluble in the water and available for pollutant adsorption from water.

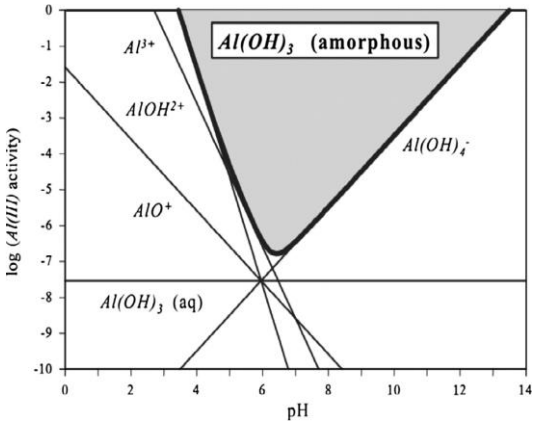

Fig. 3 Activity–pH diagram for Al^{3+} species in equilibrium with $Al(OH)_3$ (Basiri Parsa et al., 2011)

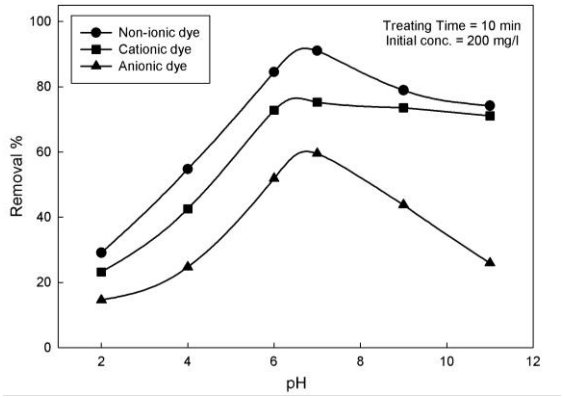

Fig. 4. Effect of initial pH on removal efficiency different dyes

Fig. 4 shows that the maximum removal efficiency for all types of dyes is achieved at pH 7. The removal efficiency remains high and almost constant in the pH range 7-11 for cationic dye due to the degradation of the dye at higher pH (Jiang et al., 2002). The lower removal efficiency at strong acidic medium is due to the higher solubility of $Al(OH)_3$ which is not useful for water treatment (Adhoum and Monser, 2004). The removal mechanism of dye molecules is based on their adsorption on the $Al(OH)_3$ flocs. There is another mechanism may be occurred in addition to simple adsorption mechanisms. The concentration of the aqueous complexes (polymeric aluminum species: $Al_3(OH)_4^{5+}$, $Al_2(OH)_2^{4+}$, $Al(OH)_2^{+}$, $AlOH^{2+}$) of the dissolved aluminum becomes maximized between pH 5-7. The aluminum atom of these species acts as an electron acceptor for an electron pair donated by different dyes (Othman and Chmielewski, 2010). These polymeric species are physicochemically/chemically reactive and they form instantaneous agglomerates with dyes as follows:

$$\text{Dye + monomeric Al} \rightarrow \text{[Dye-monomeric Al]}_{(s)}$$
$$\text{Dye + polymeric Al} \rightarrow \text{[Dye- polymeric Al]}_{(s)}$$
$$\text{Dye + Al(OH)}_{n(s)} \rightarrow \text{[Sludge]}_{(s)}$$
$$\text{[Dye-monomeric Al]}_{(s)} + \text{[Dye- polymeric Al]}_{(s)} + \text{Al(OH)}_{n(s)} \rightarrow \text{[Sludge]}_{(s)}$$

The results indicated that the order of removal efficiency for different types of dyes was as follows: nonionic > cationic > anionic. The lower adsorption of anionic and cationic dyes as charged dyes

could be attributed to a more dominant physical adsorption mechanism rather than a chemical adsorption. On the other hand, the removal efficiency increases with decreasing molecular weight. From Table 2, the adsorption of one mole of each type of dye means that the relative removal by mass was; 1 – nonionic, 2 – cationic, 2.5 – anionic.

Table 2. Chemical composition, molecular weight and type of different dyes

Type	Name	Composition	Mol.Wt
Anionic	Acid Red 1	$C_{18}N_3O_7S_2H_{13}Na_2$	493
Cationic	Basic Violet 3	$C_{25}N_3H_{30}Cl$	407
Nonionic	Disperse Blue 14	$C_{16}N_2O_2H_{14}$	266

3.2. Effect of treatment time and kinetic study

Fig. 5 shows the equilibrium concentrations for different dyes as a factor of treatment time. The rate of dye removal for different types of dyes was as follows: nonionic>cationic>anionic. It is clear that the initial dye concentration of 200 mg/L was reduced to 0.3, 1 and 2 mg/L after 60 min for nonionic, cationic and anionic, respectively. Thus, there is no significant difference between maximum removals for all types of dyes.

In order to investigate the mechanism of removal process, particularly potential rate-controlling step, the pseudo-first-order and the pseudo-second-order kinetic models were used to test the dynamic experimental data. The integrated rate law solutions for first and second order expressions are different functions but all can be written in the form of a straight line. This means that the plot of the concentration as a function of time for each expression below should yield a straight line for the correct order.

Pseudo-first-order model $$ln[C_e] = ln[C_o] - K_1 t \quad (4)$$

Pseudo-second-order model $$1/[C_e] = 1/[C_o] + K_2 t \quad (5)$$

Here, C_e is the equilibrium dye concentration at time t (the residual concentration of dye) and C_o is the initial dye concentration. The K_1 and K_2 are the rate constants for Pseudo-first-order and Pseudo-second-order models, respectively.

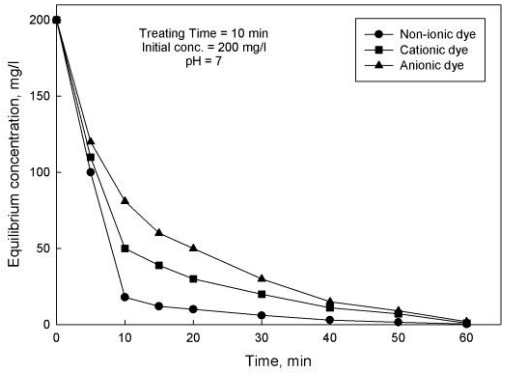

Fig. 5. Effect of time on equilibrium concentration of different dyes

Fig. 6 shows the plot of $\ln[C_e]$ versus t which gives a straight line as per pseudo-first-order adsorption kinetics which allows computation of the rate constant K_1 with high linear regression coefficient (R^2) ≥ 0.93 suggest that the dye removal process follows pseudo first-order kinetics, seen in Table 3.

Fig. 7 shows that the plot of $1/[C_e]$ versus time t gives a straight line as per pseudo-second-order adsorption kinetics which allows computation of the rate constant K_2 with very poor linear regression coefficient (R^2) of 0.51–0.58 which suggests that the dye removal process doesn't follow pseudo second-order kinetics, Table 4.

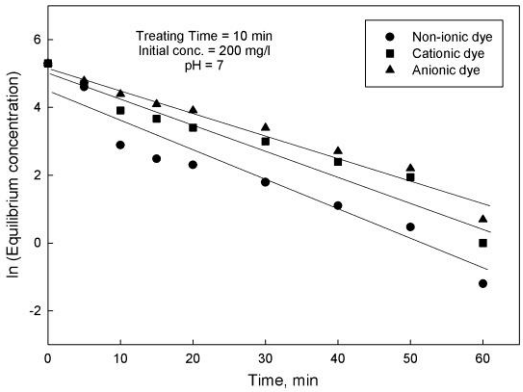

Fig. 6. Plotting of pseudo-first order model

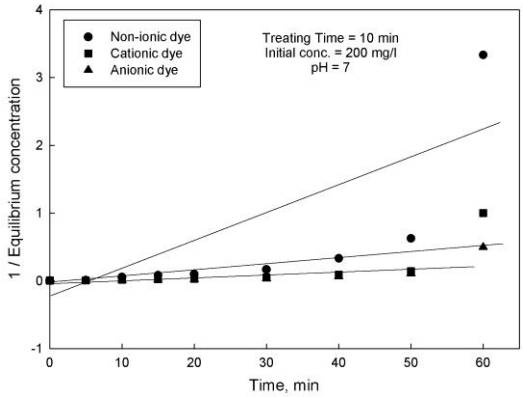

Fig. 7. Plotting of pseudo-second order model

Table 3. Pseudo-first order model constants

Item	Nonionic dye	Cationic dye	Anionic dye
R^2	0.9253	0.9411	0.9707
Intercept = ln [C_0]	4.5497	5.0224	5.2303
Slope = $-K_1$	-0.0922	-0.0734	-0.0678
K_1	0.0922	0.0734	0.0678

Table 4. Pseudo-second order model constants

Item	Nonionic dye	Cationic dye	Anionic dye
R^2	0.5543	0.5159	0.5849
Intercept = $1/C_0$	-0.4554	-0.1296	-0.0633
Slope = K_2	0.0383	0.0111	0.0058
K_2	0.0383	0.0111	0.0058

3.3. Effect of initial dye concentration and isotherm analysis

The effect of initial dye concentration on their adsorption by aluminum hydroxide floc, $Al(OH)_3$, is shown in Fig. 8. The adsorption capacities of adsorbent increased with increasing the equilibrium dye concentration, as the increasing concentration gradient overcomes the resistance to mass transfer of dye between the aqueous phase and the adsorbent (Bhattacharyya and Gupta, 2006).

The most appropriate method in designing the adsorption systems is to have an idea about the adsorption isotherm. Two equilibrium isotherm equations are used to find out the relation between

the equilibrium concentrations of the adsorbate in the liquid phase and in the solid phase. These isotherms are as follows.

3.3.1. Freundlich isotherm

Freundlich model is applied to describe a heterogeneous system characterized by a heterogeneity factor of $1/n$. This model describes reversible adsorption and is not restricted to the formation of the monolayer. It can be written as (Perez-Marin et al., 2007):

$$ln\, q_e = ln\, k_f + \frac{1}{n}(ln\, C_e), \tag{6}$$

where q_e is the amount of the dye adsorbed at the equilibrium time, C_e is the equilibrium concentration of the dye in solution. K_f is the Freundlich isotherm constant and $1/n$ is the heterogeneity factor which indicate the capacity and the intensity of the dye adsorption, respectively. The isotherm constants can be calculated from the intercept and slope of the plot between ln q_e and ln C_e.

Fig. 9 shows the fitting of results on Freundlich isotherm. The values of "n" are greater than unity which indicates the favorable nature of adsorption, Table 5. Thus, it describes a heterogeneous system characterized by physical adsorption (Demiral et al., 2008).

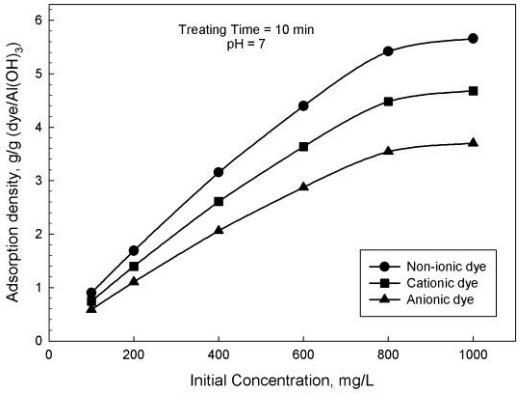

Fig. 8. Effect of initial dye concentration on the adsorption by $Al(OH)_3$

Table 5. Freundlich isotherm constants

Item	Non-ionic	Cationic	Anionic
R^2	0.9860	0.9784	0.9814
Slope (1/n)	0.4050	0.5999	0.6871
N	2.469	1.667	1.455
Intercept (ln k_f)	-0.5589	-2.0072	-2.9275
K_f	57.18×10^{-2}	13.44×10^{-2}	5.35×10^{-2}

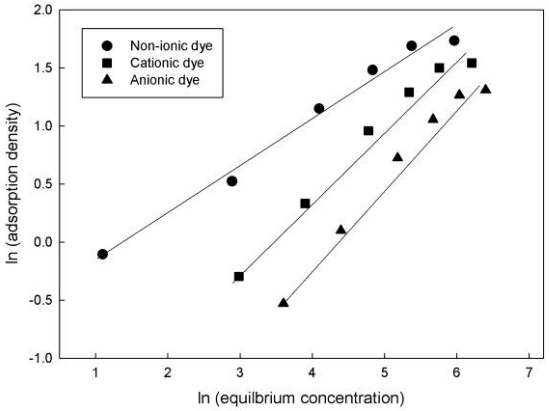

Fig. 9. Fitting of results on Freundlich isotherm

3.3.2. Langmuir isotherm

According to Langmuir model, adsorption occurs uniformly on the adsorbent and no further adsorption can take place at this site (El-Hamshary et al., 2007). The linearized form of Langmuir can be written as (Perez-Marin et al., 2007):

$$\frac{C_e}{q_e} = \frac{C_e}{q_{max}} + \frac{1}{b.q_{max}}, \tag{7}$$

where C_e is the concentration of dye in solution at equilibrium (mg/L), q_e is the amount of dye at equilibrium in unit mass of adsorbent, q_{max} and b are the Langmuir coefficient related to adsorption capacity and adsorption energy respectively. These were determined from the slope and intercept of the plot of C_e/q_e against C_e as shown in Fig. 10. The Langmuir model fits the data for all dyes. Thus, it also represents a monolayer sorption process as chemical adsorption. The maximum adsorption capacity of q_{max}, and constant are related to the binding energy of the sorption system, b. Calculated results are presented in Table 6.

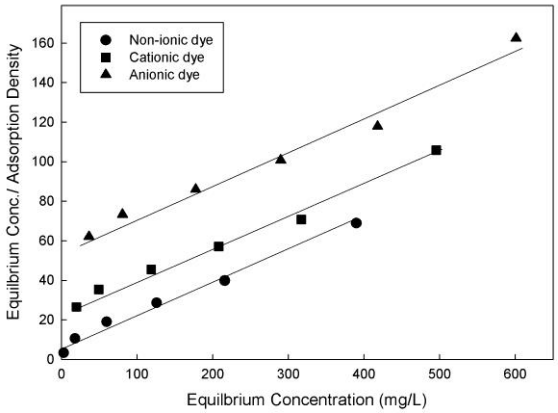

Fig. 10. Fitting of results on Langmuir isotherm

Table 6. Langmuir isotherm constants

Item	Non-ionic	Cationic	Anionic
R^2	0.9898	0.9907	0.9809
Slope ($1/q_{max}$)	0.1600	0.1579	0.1669
Intercept ($1/b.q_{max}$)	6.7259	25.0743	55.7924
q_{max} (Calculated)	6.25	6.33	5.99
q_{max} (Experimental)	5.66	4.68	3.70
b	23.79×10^{-3}	6.29×10^{-3}	2.99×10^{-3}

Table 7. The dimensionless equilibrium parameter, R_L

$b \rightarrow$	23.79×10^{-3}	6.29×10^{-3}	2.99×10^{-3}
$C_o \downarrow$	R_L		
ppm	Non-ionic	Cationic	Anionic
100	0.2959	0.6139	0.7698
200	0.1737	0.4429	0.6258
400	0.0951	0.2844	0.4554
600	0.0655	0.2095	0.3579
800	0.0499	0.1658	0.2948
1000	0.0403	0.1372	0.2506

A further analysis of the Langmuir equation can be made on the basis of a dimensionless equilibrium parameter, R_L, also known as the separation factor, given by (Demiral et al., 2008):

$$R_L = \frac{1}{(1+bC_0)}, \tag{8}$$

where b is the Langmuir constant and C_o is the initial dye concentration. Calculated R_L parameters are presented in Table 7. If the average of the R_L values for each of the different initial concentrations used is between 0 and 1, it indicates a favorable adsorption (Demiral et al., 2008).

3.4. Effect of temperature and thermodynamic study

The dependence of the removal efficiency to temperature is shown in Fig. 11. It shows that, with increasing temperature, the removal efficiency decreases. This behavior indicates that this process is an exothermic process (El-Hamshary et al., 2007).

The thermodynamic parameters; Gibbs free energy change ($\Delta G°$), enthalpy change ($\Delta H°$), and entropy change ($\Delta S°$); for the sorption of metal ions by $Al(OH)_3$ at various temperatures were calculated to evaluate the thermodynamic feasibility and the spontaneous nature of the process. The change in enthalpy ($\Delta H°$) and entropy ($\Delta S°$) were calculated using the Van't Hoff equation given in Equation 9 (Martell et al., 1977):

$$ln\, K_c = \frac{\Delta S^\circ}{R} - \frac{\Delta H^\circ}{RT}, \tag{9}$$

where $k_c = F_e/(1 - F_e)$, and $F_e = (C_o - C_e)/C_o$, T is the temperature in K, and R is the gas constant [8.314 J/mol K]. The values of $\Delta H°$ and $\Delta S°$ have been computed from the slope and the intercept of the plot of ln k_c vs. $1/T$ as seen in Fig. 12 which gives a straight line with an acceptable coefficient of determination ($R^2 \geq 0.97$), Table 8.

From the plot of $1/T$ against ln k_c, the slope is ($-\Delta H°/R$) and the intercept is $\Delta S°/R$. The values of $\Delta H°$ are -41.9, -43.3 and -48.9 kJ/mol for Nonionic, Cationic and Anionic dyes, respectively. The negative values of enthalpy changes ($\Delta H°$) suggest that the reactions are exothermic and their higher values than 40 kJ/mol, confirming extent of some chemical actions with $Al(OH)_3$ floc (Alkan et al., 2004).

The negative value of $\Delta S°$ shows decreasing randomness at the solid/liquid interface during the adsorption, indicating the adsorption was not favorable at higher temperatures.

The values of the standard Gibbs free energy change ($\Delta G°$) were estimated (Table 9) using the following equation:

$$\Delta G° = -RTlnK_c. \tag{10}$$

For nonionic dye, the values of $\Delta G°$ at all tested temperatures are negative which indicate that this adsorption process is spontaneous in nature whereby no energy input from outside of the system is required. The increase in the $\Delta G°$ with increasing temperature indicates that the process becomes less favorable at high temperatures. The values of $\Delta G°$ for cationic dye at 25 and 40°C are also negative. However, they are positive at 60 °C and above which indicate that this process is not spontaneous and energy input from outside of the system is required. On the other hand, for anionic dye, the values of $\Delta G°$ are positive at all temperatures except at 25 °C which indicate that this process is not spontaneous and becomes less favorable at high temperatures (Aksu et al., 2004).

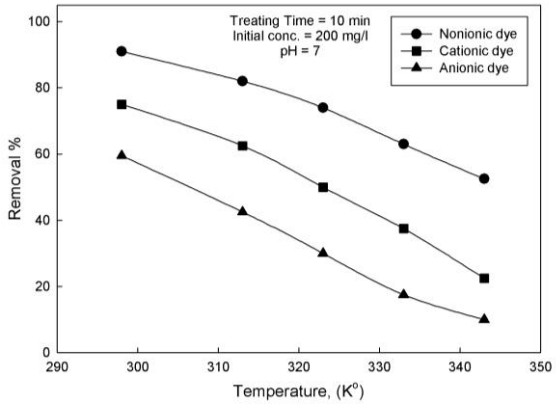

Fig. 11. Effect of temperature on the removal efficiency of different dyes

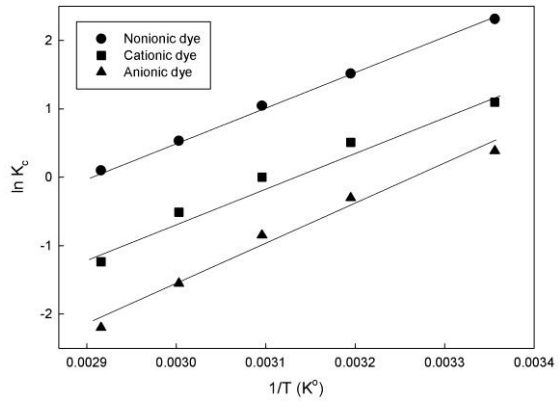

Fig. 12. Effect of temperature on the removal kinetic of different dyes

Table 8. Thermodynamic parameters; enthalpy change, Δ*H*°, and entropy change, Δ*S*°

Item	Nonionic dye	Cationic dye	Anionic dye
R^2	0.999542	0.973302	0.981375
Slope	5039	5204	5877
Intercept	-14.59	-16.23	-19.20
Δ*H*° KJ/mol	-41.9	-43.3	-48.9
Δ*S*°	-121.3	-134.9	-159.6

Table 9. Gibbs free energy change (Δ*G*°)

Temp., °C	Δ*G*°		
	Nonionic	Cationic	Anionic
25	-5732.11	-2721.86	-953.12
40	-3945.84	-1329.24	786.669
50	-2808.95	0.0000	2275.35
60	-1473.42	1414.18	4292.93
70	-285.45	3526.98	6265.75

3.5. Effect of temperature and thermodynamic study

The aim of application part is to investigate the performance of the electro-coagulation-flotation process to treat a real waste water which contains soluble dyes. Many researches proved that this process can treat synthetic solutions of some types of dyes while it is not applicable for real industrial waste water (Azam and Mohammad, 2014). In order to test its application, the wastewater from a local textile dyeing factory was used. The wastewater was treated at the optimum conditions of synthetic solutions. The natural pH of the wastewater was 8.3 so; it was adjusted to pH 7 using HCl solution before its treatment. The textile wastewater contains a mixture of dyes, iron, and zinc. Table 10 shows the evaluation of treated wastewater at an operating voltage of 30 V and at an electric current of 1 A for 10 minutes at pH 7 and 25 °C. The floated gelatinous aluminum hydroxide flocs with adsorbed pollutants was collected and filtered using fast filter paper the dried to reduce its amount to a very small quantity.

The electrical energy consumption *E* is calculated by following equation (Patil et al., 2011):

$$E = \frac{U \times I \times t}{V} \times 10^{-3}, \tag{11}$$

where *U* is the operating voltage (volt), *I* is the operating current (amperes), *t* is the time of treatment (hours), and *V* is the volume of wastewater (m^3). The process of electro-coagulation-flotation was also performed on samples of real textile effluent.

The removal efficiency was ranging between 92-99% for all constituents. The energy consumption amounts to 0.0167 kWh per liter of treated wastewater.

Table 10. Evaluation of textile effluent before and after treatment using electro-coagulation-flotation

Item	Untreated	Treated	Removal %
pH	8.3	8.6	--
TS, mg/dm^3	4592	183	96
TSS, mg/dm^3	286	2.85	99
COD	963	77	92
BOD	132	10.5	92
Color %	32	0.96	97
Fe	3.1	0.12	96
Zn	1.2	0.05	96
Turbidity (NTU)	279	2.7	99

4. Conclusions

Electro-coagulation-flotation of different dye types from aqueous solutions and a real textile wastewater showed that, the maximum dye removal was achieved at pH 7. The order of the dye removal is nonionic>cationic>anionic. The removal process follows pseudo first-order kinetics. Freundlich and Langmuir isotherm models indicate that the adsorption is characterized by physical and chemical adsorptions. The dimensionless equilibrium parameter, R_L values were between 0 and 1, indicating favorable adsorption. The negative values of enthalpy changes ($\Delta H°$) suggest that the reactions are exothermic with values than 40 kJ/mol. This confirms the presence of chemical interactions with $Al(OH)_3$ floc. The negative values of entropy change ($\Delta S°$) and Gibbs free energy change ($\Delta G°$) indicate decreasing randomness at the solid/liquid interface during the adsorption while this process is spontaneous which need energy input from outside of the system. The increase in the $\Delta G°$ with increasing temperature indicates that the process becomes less favorable at high temperatures.

Treatment of a real wastewater from textile dyeing factory at optimum conditions of 30 Voltage, 1 Ampere, pH 7 and 25 °C for 10 minutes, showed that the removal efficiency was ranging between 92-99% for all constituents. The energy consumption was 0.0167 kWh/dm^3.

References

ABDEL KHALEK, M.A., PAREKH, B.K., 2003. *Separation of ultra-fine wood particles from waste water to prevent water pollution*. Afinidad, 60(503), 71-75.

ADHOUM, N., MONSER, L., 2004. *Decolourization and removal of phenolic compounds from olive mill wastewater by electrocoagulation*. Chemical Engineering and Processing, 43, 1281-1287.

AHMED, S.N., SHREESHIVADASAN, C., ZURIATI, Z., SAAD, A.A., 2015. *Treatment Performance of Textile Wastewater Using Electrocoagulation Process under Combined Electrical Connection of Electrodes*. Int. J. Electrochem. Sci., 10, 5924-5941

AKSU, Z., KABASAKAL, E., 2004. *Batch adsorption of 2,4-dichlorophenoxy-acetic acid (2,4-D) from aqueous solution by granular activated carbon*. Sep. Purif. Technol., 35, 223–240.

ALKAN, M., DEMIRBAS, O., CELIKCAPA, S., DOGAN, M., 2004. *Sorption of acid red 57 from aqueous solution onto sepiolite*. J. Hazard. Mater., 116, 135–145.

AL-SHANNAG, M., LAFI, W., BANI-MELHEM, K., GHARAGHEER, F., DHAIMAT, O., 2012. *Reduction of COD and TSS from Paper Industries Wastewater Using Electro-Coagulation and Chemical Coagulation*. Sep. Sci. Technol., 47(5), 700.

APHA, 1992. *Standard Methods for Examination of Water and Wastewater*. 17th Ed. Washington DC.

AZAM, P., MOHAMMAD, E.O., 2014. *Removal of Dye from Industrial Wastewater with an Emphasis On Improving Economic Efficiency and Degradation Mechanism*. Journal of Saudi Chemical Society, 6, 1–8.

BASIRI PARSA J., REZAEI VAHIDIAN, H., SOLEYMANI, A.I.R., ABBASI, M., 2011. *Removal of Acid Brown 14 In Aqueous Media by Electrocoagulation: Optimization Parameters and Minimizing of Energy Consumption*. Desalination, 278, 295-302.

CHEN, G., 2004. *Electrochemical Technologies in Wastewater Treatment*. Separation and Purification Technology, 38(1), 11-41.

CLECERI, L.S., GREENBERG, A.E., EATON, A.D., 1998. *Standard Methods for the Examination of Water and Wastewater*. 20th Ed., American Public Health Association, USA, Washington DC.

CRINI, G., 2006. *Non-Conventional Low-Cost Adsorbents for Dye Removal*: *A Review*. Bioresour. Technol., 97, 1061.

DEMIRAL, H., DEMIRAL, I., TUMSEK, F., KARABACAKOGLU, B., 2008. *Adsorption of Chromium (VI) From Aqueous Solution by Activated Carbon Derived from Olive Bagasse and Applicability of Different Adsorption Models*. Chem. Eng. J., 144, 188-196.

EL-HAMSHARY, H., EL-SIGENY, S., 2007. *Removal of Phenolic Compounds Using (2-Hydroxyethyl Methacrylate/ Acrylamidopyridine) Hydrogel Prepared by Gamma Radiation*. Sep. Purif. Technol., 57, 329–337.

ELKSIBI, I., HADDAR, W., TICHA, M.B., GHARBI, R., MHENNI, M., 2014. *Development and Optimization of a Nonconventional Extraction Process of Natural Dye from Olive Solid Waste Using Response Surface Methodology (RSM)*. Food Chem., 161, 345-352.

GARG, V.K., AMITA, M., KUMAR, R., GUPTA, R., 2004. *Basic Dye (Methylene Blue) Removal from Simulated Wastewater by Adsorption Using Indian Rosewood Sawdust: A Timber Industry Waste.* Dyes and Pigments, 63(3), 243-250.

HUNSOM, M., PRUKSATHORNA, K., DAMRONGLERDA, S., VERGNESB, H., DUVERNEUILB, P., 2005. *Electrochemical Treatment of Heavy Metals (Cu^{2+}, Cr^{6+}, Ni^{2+}) From Industrial Effluent and Modeling of Copper Reduction*. Water Res., 39, 610-616.

JIANG, J., GRAHAM, N., ANDRE, C., KELSALL, G.H., BRANDON, N., 2002. *Laboratory Study of Electro-Coagulation–Flotation for Water Treatment*. Water Res., 36, 4064-4078.

KONSTANTINOS, D., ACHILLEAS, C., EVGENIA, V., 2011. *Removal of Nickel, Copper, Zinc and Chromium from Synthetic and Industrial Wastewater by Electro-Coagulation*. International Journal of Environmental Science, 1(5), 697-710.

BHATTACHARYYA, K.G., GUPTA, S.S., 2006. *Adsorption of Fe(III) from water by natural and acid activated clays: Studies on equilibrium isotherm, kinetics and thermodynamics of interactions*. Adsorption, 12, 185–204.

LEMLIKCHI, W., KHALDI, S., MECHERRI, M.O., LOUNICI, H., DROUICHE, N., 2012. *Degradation of Disperse Red 167 Azo Dye by Bipolar Electrocoagulation*. Sep. Sci. Technol., 47(11), 1682.

MAHMOODI, N.M., ARAMI, M., 2009. *Numerical Finite Volume Modeling of Dye Decolorization Using Immobilized Titania Nanophotocatalysis*. Chem. Eng. J., 146(2), 189–193.

MARTELL, A.E., SMITH, R.M., 1977. *The Oxidation of Cobalt (II) Adsorbed On Manganese Dioxide*. Cosmochim. Acta., 43, 781–787.

MOHORA, E., RONCEVIĆ, S., DALMACIJA, B., AGBABA, J., WATSON, M., KARLOVIĆ, E., DALMACIJA, M., 2012. *Removal of Natural Organic Matter and Arsenic from Water by Electrocoagulation/Flotation Continuous Flow Reactor*. J. Hazard. Mater., 2(6), 257-264.

MORSI, M.S., AL-SARAWY, A.A., SHEHAB EL-DEIN, W.A., 2011. *Electrochemical Degradation of Some Organic Dyes by Electrochemical Oxidation On a Pb/Pbo_2 Electrode*. Desal. Water Treat., 26(1–3), 301.

MUTHUKUMAR, M., GOVINDARAJA, M., MUTHUSAMY, A., RAJU, G.B., 2010. *Comparative Study of Electro-Coagulation and Electro-Oxidation Processes for The Degradation of Ellagic Acid from Aqueous Solution*. Sep. Sci. Technol., 46(2), 272.

NANDI, B.K., PATEL, S., 2017. *Effects of Operational Parameters On The Removal Of Brilliant Green Dye From Aqueous Solutions By Electrocoagulation*. Arabian J. Chem., 10, S2961-S2968.

OTHMAN, A.H., CHMIELEWSKI, H. J., 2010, *Materials Useful in Making Cellulosic Acquisition Fibers in Sheet Form*. Patent EP1675556A4, Rayonier Prod & Fncl Serv Co.

PATIL, B.N., NAIK, D.B., SHRIVASTAVA, V.S., 2011. *Photocatalytic Degradation of Hazardous Ponceau-S Dye from Industrial Wastewater*. Desalination, 269(1–3), 276–283.

PEREZ-MARIN, A.B., MESEGUER ZAPATA, V., ORTUNO, J.F., AGUILAR, M., SAEZ, J., LLORENS, M., 2007. *Removal of cadmium from aqueous solutions by adsorption onto orange waste*. J. Hazard. Mater., B139, 122–131.

PIRKARAMIA, A., OLYA, M.E., LIMAEE, N.Y., 2013. *Decolorization of Azo Dyes by Photo Electro Adsorption Process Using Polyaniline Coated Electrode*. Prog. Org. Coat., 76, 682–688.

SAHU, O., MAZUMDAR B., CHAUDHARI, P.K., 2014. *Treatment of Wastewater by Electrocoagulation: A Review*. Environ. Sci. Pollut. Res., 21, 2397-2413.

CHATURVEDI, S.I., 2013. *Electrocoagulation: A Novel Waste Water Treatment Method*. International Journal of Modern Engineering Research (IJMER), 3(1), 93-100.

SHAH, V., MADAMWAR, D., 2013. *Community Genomics: Isolation, Characterization and Expression of Gene Coding for Azoreductase*. Int. Biodeter. Biodegrad., 79(4), 1–8.

SLEIMAN, M., VILDOZO, D., FERRONATO, C., CHOVELON, J.M., 2007. *Photocatalytic Degradation of Azo Dye Metanil Yellow: Optimization and Kinetic Modeling Using a Chemometric Approach*. Appl. Catal. B: Environ., 77(1-2), 1–11.

THIRUGNANASAMBANDHAM, K., SIVAKUMAR, V., MARAN, J. P., 2014. *Efficiency of Electrocoagulation Method to Treat Chicken Processing Industry Wastewater - Modeling and Optimization*. J. Taiwan Inst. Chem. Eng., 45, 2427-2435.

THIRUGNANASAMBANDHAM, K., SIVAKUMAR, V., MARAN, J.P., 2013. *Optimization of Electrocoagulation Process to Treat Biologically Pretreated Bagasse Effluent*. J. Serb. Chem. Soc., 78, 613-626.

VASUDEVAN, S., OTURAN, M.A., 2014. *Electrochemistry: As Cause and Cure in Water Pollution–An Overview*. Environ. Chem. Lett., 12, 97-108.

VILLE, K., TOIVO, K., JAAKKO, R., ULLA, L., 2013. *Recent Applications of Electrocoagulation in Treatment of Water and Wastewater*. Green and Sustainable Chemistry, 3, 89-121.